World Journal of
Advanced Science and Tehnology

Journal homepage: https://zealjournals.com/wjast/

(RESEARCH ARTICLE)

Synthesis, characterization, and pharmacological evaluation of dextrin capped cadmium sulfide quantum dots conjugated with temozolomide for drug delivery and imaging application

Lourdes Rodríguez-Fragoso [1, *], Erick Ayala-Calvillo [1], Frida Leo-Campos [1], Gerardo González de la Cruz [2], Patricia Rodríguez [2] and Alfonso Leija Salas [3, *]

[1] *Faculty of Pharmacy, Autonomous University of the State of Morelos, Cuernavaca 62210, Mexico.*
[2] *Department of Physics, CINVESTAV - I.P.N. PO Box 14-740, 07000. Mexico City, Mexico.*
[3] *Center for Genomic Sciences, National Autonomous University of Mexico, Av. Universidad 2001 Col. Chamilpa, CP62210, Cuernavaca, Morelos, Mexico*

World Journal of Advanced Science and Technology, 2023, 03(02), 027–037

Publication history: Received on 10 July 2023; revised on 26 August 2023; accepted on 28 August 2023

Article DOI: https://doi.org/10.53346/wjast.2023.3.2.0066

Abstract

Quantum dots (QDs) of cadmium sulfide semiconductor capped with dextrin and bioconjugated with temozolomide (CdS/Dx+TMZ) were used to target and provide imaging of glioma cells. CdS/Dx+TMZ QDs were in the range of 6.5 nm in size and exhibited an intense fluorescence emission in the green spectrum, which allowed us to monitor fluorescence imaging in a rat glioma cell line. The results showed that glioma cells efficiently took up the CdS/Dx+TMZ QDs, which had a large accumulation time in cells and were distributed in both the cytoplasm and nucleus, where the pharmacological drug effects were enhanced. CdS/Dx+TMZ QDs were more cytotoxic than TMZ and CdS/Dx alone. Glioma cells treated with 100 µM CdS/Dx+TMZ QDs showed both an increase in size (cytoplasm and nucleus) and in the number of cell deaths by apoptosis. The morphological analysis showed the presence of binucleated cells and membrane blebbing, as well as apoptotic bodies. This study confirmed the effective cellular uptake of CdS/Dx QDs bioconjugated with TMZ and their pharmacological effects in a glioma cell line. Our conclusion is that CdS/Dx+ TMZ QDs could be simultaneously used as drug delivery and cell monitoring system for the treatment of GBM and other brain tumors.

Keywords: CdS/Dx; Temozolomide; Glioblastoma; Pharmacological evaluation

1 Introduction

Nanocarrier drug delivery has been employed successfully in recent years; however, certain challenges regarding successful delivery to target sites remain [1-3]. The goal of designing drug nanocarriers is to reach the target more efficiently and increase efficacy, thereby reducing toxicity. In this sense, the pharmaceutical industry and related research have focused on developing novel nanoformulations for more than a decade. Thanks to this work, we now know that several issues must be considered in the design of nanocarriers, including their chemical, physical, and morphological characteristics, optical profile, and capping agents. All this will influence potential interactions between biomolecules, cellular components or drugs, as well as the effectiveness the desired application (cell detection, imaging or drug delivery) [4-6].

From the pharmaceutical point of view, the construction of a nanoformulations entails a new pharmacological profile (i.e., new chemical structures, novel three-dimensional shapes, new molecular weight) that will affect the phases of pharmacological action (the pharmaceutical, pharmacokinetic and pharmacodynamic phases). This necessitates

* Corresponding author: Lourdes Rodríguez-Fragoso

physicochemical, optical and morphological characterization, as well as information regarding biocompatibility and pharmaceutical profile.

Quantum dots (QDs) are nanomaterials with photoluminescent properties. They have proved an excellent probe in biomedicine given their physical, chemical and optical properties. The great coupling between QDs and drugs means that, today, the first are used as a tool for improving drug release in target sites while their photoluminescence allows us to follow the complex nanocarrier-drug into the cell [7-9]. The development of bioconjugated QDs has helped to improve their biocompatibility at the same time it has allowed us to access intracellular sites more efficiently, thus improving therapeutic effectiveness [10-12].

Temozolomide (TMZ) is an alkylating agent that introduces methyl groups into cellular DNA, leading to apoptosis, senescence, or cell cycle arrest in cancer [13, 14]. For many years, this drug has been the "gold standard" and treatment of choice for patients with brain tumors, particularly those with glioblastoma (GBM) [15, 16]. TMZ has some pharmaceutical advantages compared to other alkylating agents: it is a small lipid- soluble molecule that easily crosses the blood-brain barrier (BBB) and can easily reach nervous tissue. Unfortunately, and as is well known, TMZ undergoes spontaneous hydrolysis and generates an active metabolite that can affect drug-cell membrane interaction, reducing therapeutic effectiveness [17]. Therefore, many researchers are focusing on finding new nanoformulations that allow for more efficient drug delivery while reducing the problems that affect therapeutic effectiveness [18].

In the past decade, this research group has focused on synthesizing and characterizing cadmium sulfide quantum dots passivated with polymers to protect the cadmium core and reduce its toxicity (CdS/dextrin, CdS/maltodextrin) [19-22]. These QDs have been shown to be biocompatible, capable of crossings biological barriers and having a wide tissue distribution with a variable mean residence time (MTR) in each organ [23].

They are taken up at the cellular level and distributed not only into the cytoplasm but also inside the nuclei of most of the studied cell lines. The development of CdS/dextrin QDs conjugated with drugs has been recently initiated and the QDs have been shown to be effective nanotransporters with more efficient drug delivery to the cell and, thus, an improvement in pharmacological effectiveness [24]. The main purpose of this work was to bioconjugate the CdS/Dx QDs with TMZ and carry out an optical characterization of these QDs using different methods, as well as provide an evaluation of their pharmacological effect at the cellular level.

2 Materials and Methods

Cadmium chloride (CdCl2, 99.9% pure), potassium hydroxide (KOH, semiconductor grade), ammonium nitrate (NH4NO3, 99% pure), thiourea (CS(NH2)2, 99% pure), sodium hydroxide (NaOH, 99% pure), dextrin ((C6H10O5)n, 99% pure) 1,1–carbonyldiimidazole ((C3H3N2)2CO, 97% pure), tetrahydrofuran (THF) (C4H8O, 99.9 % pure) and MTZ (C6H6N6O2, 98% pure) were all purchased from Sigma-Aldrich. Dilute aqueous solution of 1 M NaOH was used to control the pH of the synthesis and employed in the bioconjugation process to buffer the carbonates at pH 9 (0.1 M). Finally, deionized water was used as solvent.

2.1 Synthesis of the CdS/Dx QDs

Colloidal CdS/Dx QDs were produced by chemical synthesis process via aqueous solutions: $CdCl_2$ (0.02 M), KOH (0.5 M), NH_4NO_3 (0.5 M) and $CS(NH_2)_2$ (0.2 M) were mixed and heated at 75°C. Dextrin was used as a capping agent at 2% concentration. To control the formation of the QDs during the synthesis of the CdS/Dx QDs, these solutions were added in a balloon flask and adjusted to pH 11 by adding drops of 1M NaOH solution, maintaining 80° temperature with stirring, for 40 min. After the synthesis, the yellow precipitate was centrifuged at 13 000 rpm for 30 min. Finally, the yellow precipitate, CdS/Dx QDs, was washed 6 times with deionized water and acetone and finally dried at 40° for 24 h [19].

2.2 Bioconjugation of CdS/Dx QDs with temozolomide

The CdS/Dx+TMZ QDs were formed by dispersing 8 mg of freshly prepared CdS/Dx QDs suspended in 10% THF containing carbonyldiimidazole (CDI) at a concentration 0.1 M and mixing it for several minutes. After three more washes were performed, centrifuging with THF at 14,000 rpm was carried out every 15 minutes. The mix was washed again with cold water (4°C) and centrifuged at 14 000 rpm for 30 min; the supernatant was removed. Then, 32mg of TMZ were dissolved in PBS and added to the CdS/Dx QDs. The mixture was stirred to 700 rpm for 24 h at room temperature. Finally, the solution was washed three times with PBS and centrifuged at 14 000 rpm for 30 min. The pellets were washed with fresh buffer and the CdS/Dx+TMZ QDs were dried at 37°C for 24 h.

2.3 Optical characterization of CdS-Dx/TMZ QDs

The X-ray diffraction (XRD) pattern provides information about the structure and size of the crystalline CdS/Dx+TMZ QDs, which was determined on an X-ray diffractometer (Siemens D5000, Cu Kα radiation). The hydrodynamic diameter distribution of the CdS/Dx+TMZ QDs was performed on a dynamic light scattering (DLS, model Nanotrac Wave, Microtrac Inc., USA). The Fourier-Transform-Infrared spectroscopy (FTIR) is a method to determine the linkage of the TMZ molecule on the CdS/Dx QDs in the conjugation technique. The spectrum was recorded on a FTIR spectrometer (Model Nicolet 6700, Thermo Scientific) and transmission bands in the range of 400-4000 cm^{-1} wavelengths with 180 sec scanner time. An XE-Bio Atomic Force Microscope (Park Systems Co., Suwan, Korea) was used to obtain topographic images of QDs bioconjugates. We used XEP and XEI software from Park Systems to analyze the data. PPP-NCHR silicon nitride cantilevers with nominal spring constant of 60 nN/m from nanosensors were used in non-contact mode. DNP-S-D C and D silicon nitride cantilevers with nominal spring constant of 0.06 N/m (Bruker, USA) were used in Contact mode. The DNP-S-D cantilevers were calibrated using the Thermal Method routine built into the XEI software. Topographic representations were obtained at 21 ± 1°C. Scans performed in Contact mode were carried out at load forces lower than 1 nN. The images shown correspond to one typical sample.

2.4 Cell culture and cell viability assay

C6 glioma cells lines (ATCC CCL-107) were cultured in Dulbecco's modified Eagle's medium (DMEM, GIBCO, MA, USA) supplemented with 10% fetal bovine serum (GIBCO, MA, USA). Cells were grown at 37 °C under a 5% CO2 atmosphere and 90% humidity. Cell viability and cell proliferation rate were determined using a MTT (methyl tetrazolium, Sigma-Aldrich USA) assay [25]. Briefly, for cell viability, C6 cells were plated in a 96-well plate (10,000/well) and kept for 24 h at 37oC and 5% CO2. The medium was changed, and the cells treated with CdS/Dx QDs alone [10 and 100 μM], TMZ [100 μM] as well as CdS/Dx QDs bioconjugated with TMZ [10 and 100 μM]; cells were kept alive for 24, 48, 72 and 96 h. After treatment, the medium was gently replaced with 20 μL MTT (5mg/mL) and 150 μL of medium and kept at 37oC for 4 h. The medium was replaced again by addition of 200 μL DMSO and 25 μL Sorensen's glycine buffer (glycine 0.1 M, NaCl 0.1 M, pH 10.5). Cell viability was determined by measuring optical absorbance on a microplate reader (Bio-Rad) at 590 nm. We included untreated cells as control.

2.5 Fluorescent microscopic visualization of fluorescence of CdS-Dx/QDs in C6 cells

C6 cells were employed to confirm the selective absorption of CdS/Dx QDs, both on their own and bioconjugated with TMZ. The cells (50,000/well) were placed on a sterile coverslip in a 12-multiwell. The cells were incubated for 24 h, rinsed with buffer solution and then treated with CdS/Dx QDs [10 and 100μM], TMZ [100 μM] and CdS/Dx +TMZ [10 and 100μM] for 24 h. After rinsing with cold buffer solution, the cells were set for 20 min in 200 μL of 4% paraformaldehyde and later rinsed again with buffer solution. Set cells were protected with a glass slide with 50% glycerol/PBS (v/v) and visualized on a microscope (Nikon Al, Nikon, Japan). QDs were stimulated with a 488 nm laser, and their waves collected at 680 nm. To track the subcellular localization of CdS/Dx+TMZ QDs, cells were observed under confocal epifluorescence microscopy.

2.6 Assessment of cell death by fluorescence microscopy

The assessment of cell death was carried out using the acridine orange and ethidium bromide staining assay as previously described [26]. Briefly, the C6 cells were seeded into a 6-well plate (300,000/well) and incubated for 24h at 5% CO2 and 37°C. The culture medium was replaced with a fresh one containing CdS/Dx QDs [10 and 100μM], TMZ [100 μM] or CdS/Dx+TMZ [10 and 100μM]. The cells were then incubated for another 24 h. After washing thoroughly with DPBS, 250 μL of a mixture of 100 μg/mL acridine orange/100 μg/mL ethidium bromide (AO/EB) (Sigma Aldrich, USA) was added to each well. The cells were then incubated at room temperature for 10 seconds and observed under a fluorescence microscope. Images of fluorescently stained cells were photographed with an Olympus digital camera. Cells incubated in culture medium were used as a non-treated control. 1μL/mL of 30% H_2O_2 served as apoptosis control and smashed up cells were used as necrosis control. Cells were categorized as healthy (fluorescent green cells without any nuclear staining), apoptotic (condensed or fragmented orange red nucleus) or necrotic (red, or patchy nucleus).

2.7 Statistical analysis

Results were expressed as mean ± standard deviation of 3 determinations. Results were statistically analyzed using the SPSS 10.0 program (SPSS Inc., Chicago, Ill., USA), the student t test, and ANOVA. Variances were considered significant if the P-value was less than 0.05.

3 Results

3.1 Synthesis and characterization of CdS/Dx QDs bioconjugated with temozolomide

The XRD spectrum of pure temozolomide (Fig. 1A) is characterized by sharp diffraction peaks at different values of 2θ, which could be indexed to scattering from different planes associated with the chemical structure of TMZ [16]. The XRD spectrum of the CdS/Dx QDs shown in Fig. 1b exhibited prominent broad peaks at 2θ values of 26.5°, 44° and 52.13°, which were consistent with the diffraction peaks of CdS planes in cubic phase seen in other studies [13, 27]. The same characteristic peaks can also be found in the spectrum of CdS/Dx+TMZ QDs in Fig. 1c. The peaks corresponding to the reflection plane around 2θ=26.3°, 28.6°, and 29.7 are predominantly attributed to the presence of TMZ molecule. These XRD results evidenced the presence of TMZ on CdS/Dx QDs after conjugation.

The FTIR spectrum of dextrin with the main peaks identified by arrows is shown in Fig. 2a. For pure dextrin, the peak at 3399 cm-1 is due to the stretching vibrations of O-H; a small peak at 2925 cm^{-1} is attributed to the C-H stretching vibrations. The peaks at 1457, 1423 and 1369 cm^{-1} are associated to H-C-OH δ vibrations, the bands at 1159 is assigned to C-O-C stretching vibrations, and 1025 cm^{-1} is assigned to C-O vibrations. The FTIR spectrum of the CdS/Dx QDs (Fig. 3b) exhibited the same line positions as in Fig. 3a, except that there was an additional peak as compared to pure dextrin at 2001 cm-1 due to C-N stretching vibrations because of the thiourea used in the synthesis of the CdS nanoparticles. The FTIR spectrum of pure TMZ (Fig. 3c) showed peaks at 3421,3388, 3390 and 1600 cm^{-1} associated to NH vibrations; the peaks at 1758,1731, and 1679 cm-1 are associated to C=O vibrations. The absorption band at 1364 cm^{-1} is assigned to the N-H bending vibrations for the primary amine structure. The FTIR spectrum of CdS/Dx + TMZ QDs (Fig. 3d) showed a broad peak at 3353 cm^{-1} because of the O-H and N-H overlap stretching vibrations. The absorption peak observed at 2913 cm^{-1} is assigned to C-H and CH2 vibrations. The peak in 1997 is assigned to C-N stretching vibrations because of the thiourea employed in the synthesis of the CdS nanoparticles. The absorption peak at 1429 and 1371 were assigned to H-C-OH vibrations, the peak at 1149 was assigned to C-O-C vibrations and the last peak at 1022 was assigned to C-O vibrations. The peak at 2001 cm^{-1} in CdS/Dx QDs decreases in intensity as compared to the conjugated CdS/Dx QDs FTIR spectrum. These FTIR results suggest that the attachment of TMZ to the CdS-Dx QDs occurred via the interaction of amine groups of the TMZ with the carboxamide group. The topographic morphology of CdS/Dx + TMZ QDs was examined using AFM. Figure 3 show the typical surface topography and surface homogeneity images of CdS/Dx QDs bioconjugated with TMZ. The reduction in the number of QDs due to an increase in the size of CdS/Dx + TMZ QDs was evident. No surface roughness was observed in CdS/Dx + TMZ QDs. The Cd/-Dx + TMZ QDs were generally over 6.5 nm in diameter, whereas the plain CdS/Dx QDs were smaller (3.5 nm).

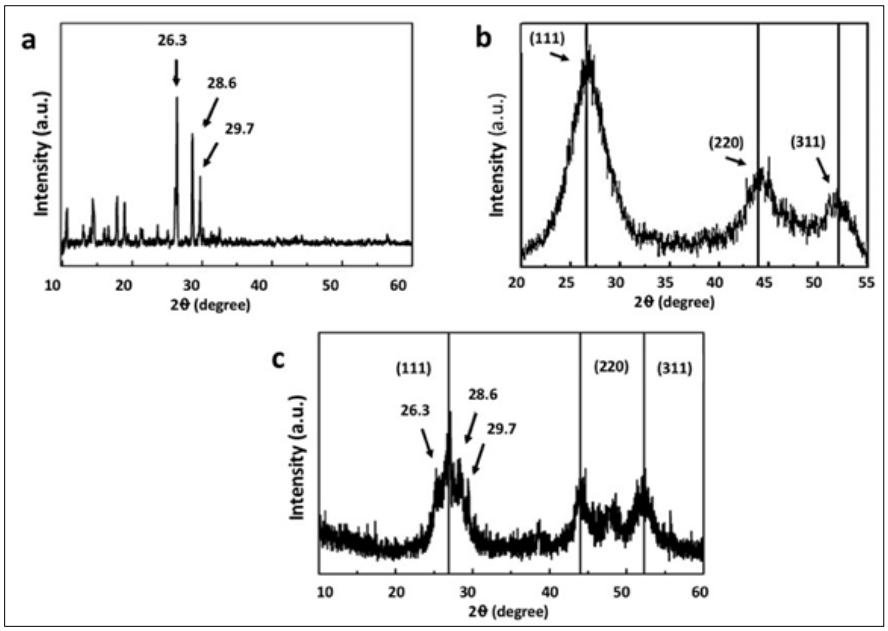

Figure 1 Standard XRD pattern of (A) pure temozolomide, (B) CdS/Dx QD synthesized nanoparticles, and (C) CdS/Dx+TMZ QD bioconjugated nanoparticles. All the samples were dried as powder at room temperature

3.2 Effect of CdS-Dx + TMZ QDs on cell viability

Figure 4 shows the effect of CdS/Dx + TMZ QDs [10 and 100 μM] at different times on the viability of C6 cells. As we can see, the effect of CdS/Dx + TMZ QDs [100 μM] on cell viability started at 48 h, with QDs reducing it in 30% ($p<0.05$), whereas TMZ alone produced the same effect until 72 h later (30%, $p<0.05$). CdS/Dx + TMZ QDs [10 μM] and TMZ alone reduced cell viability at 72 and 96 h, by 30-35% respectively, as compared to control group ($p<0.05$). CdS/Dx +TMZ QDs at 100 μM reduced cell viability more significantly at 72h, 31% as compared to TMZ group ($p<0.05$), whereas at 96 h, the inhibition of cell viability was 42% as compared to TMZ group ($p<0.05$). It is important to mention that CdS/Dx QDs [100 μM reduced 8-10% cell viability at 72 and 96 h ($p<0.05$).

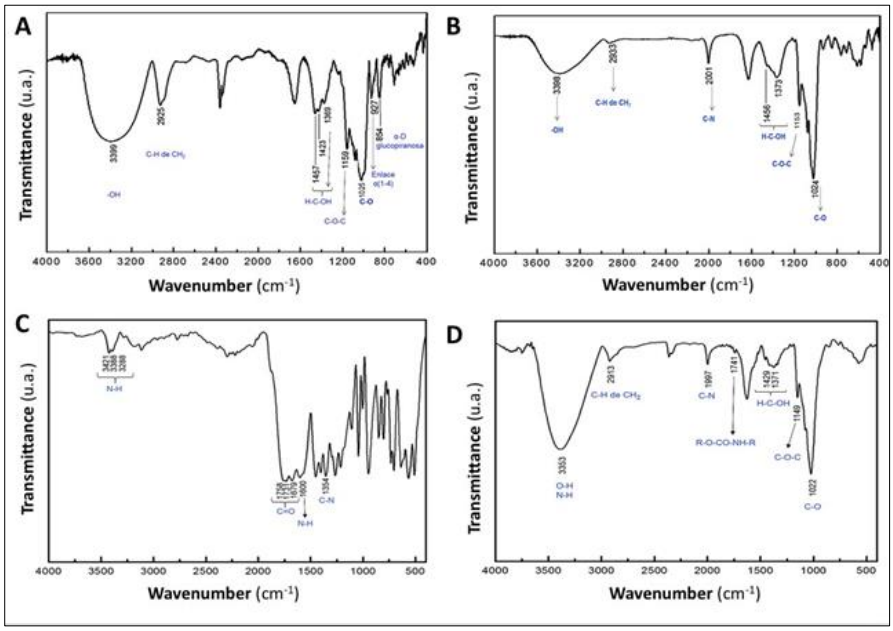

Figure 2 Typical FT-IR spectra of the powder sample of (A) pure dextrin, (B) CdS/Dx QD synthesized nanoparticles, (C) pure temozolomide, and (D) CdS/Dx+TMZ QD bioconjugated nanoparticles. All at room temperature from 4000–400/500 cm^{-1}

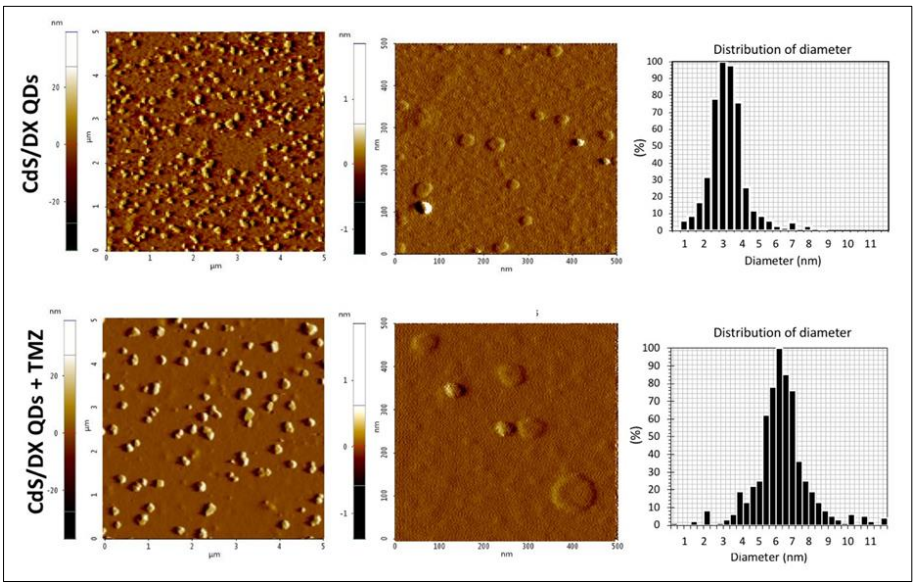

Figure 3 AFM images (height and three-dimensional) of CdS/Dx QD synthesized nanoparticles, and CdS/Dx+TMZ QD bioconjugated nanoparticles, with their corresponding particle size distribution of 3.5 nm and 6.5 nm for CdS/Dx+TMZ QDs and CdS/Dx+TMZ QDs, respectively

Fig. 4 Effect of CdS/Dx+TMZ QDs on cell viability of C6 glioma cells lines. Cells were exposed in cultured medium with plain CdS/Dx QDs [10 and 100 μM], TMZ [100 μM], and CdS/Dx QDs bioconjugated with TMZ [10 and 100 μM] nanoparticles at different times (24h, 48h, 72h, and 96h). Results are expressed as percentage of cell viability as compared to control group. Data are presented as the mean ± SD of at least three independent experiments. *p <0.05 as compared to control group; * p<0.05 as compared to CdS/Dx [100 μM]; # p<0.05 as compared to TMZ [100 μM]; & p<0.05 as compared to CdS/Dx+TMZ [10 μM]

3.3 Fluorescent microscopic visualization of the light emission of CdS/Dx + TMZ QDs in C6 cells

The fluorescent properties of CdS/Dx + TMZ QDs allows us to monitor their uptake and cell distribution under a fluorescent microscope and as shown in Figure 5. C6 cells were incubated with 100 μM of CdS/Dx + TMZ QDs during 72 h and washed to remove all unbound QDs. In untreated C6 cells and those treated with CdS/Dx QDs, the cellular morphology was the usual for these cells, as evidenced by Giemsa stain. Cells treated with TMZ alone and bioconjugated with CdS/Dx QDs presented cell death and enlarged size with double nuclei (Figure 5a). The analysis of light emission revealed that cells treated with CdS/Dx QDs emitted green colored fluorescence in the cytoplasm and, in a lesser amount, in the nucleus; cell morphology was quite similar to that of control cells (Figure 5b). However, cells treated with TMZ alone or conjugated with QDs at 100 μM showed higher sizes (in cell and nucleus) and, in addition, there were multiple cells that showed membrane blebbing and apoptotic bodies. Those effects were more evident in cells treated with CdS/Dx + TMZ QDs. An analysis of cells under fluorescent microscope evidenced that the intensity of light emission was distributed homogeneously in both the cytoplasm and nucleus of cells treated with CdS/Dx + TMZ QDs, whereas those treated with QDs alone had light emission mainly in the cytoplasm. The light emission was higher in the nuclei of cells treated with CdS/Dx + TMZ QDs than in cells treated with QDs alone. These results show that CdS/Dx + TMZ QDs can reach the nucleus and produce pharmacological effects.

Characterization of cell death induced by of CdS/Dx + TMZ QDs in C6 cells Because CdS/Dx + TMZ QDs at 100 μM produced a significant reduction in cell viability after 48 h and onward, we decided to do another assay to characterize the type of cell death induced by CdS/Dx + TMZ QDs [100 μM] at 72h. For this case, we used double staining (AO/EtBr) to differentiate between apoptotic and necrotic cells. Figure 6 shows positive control by apoptosis (cells treated with H2O2) and necrosis (crushed cells). We found a reduced number of cells and the presence of cell death by apoptosis (49%) in cells treated with CdS/Dx + TMZ QDs at 72 h, as compared with control group (p<0.05). Cells treated with TMZ alone [100 μM] during 72 h showed cell death by apoptosis (26%) but also a greater number of cells when compared with the CdS/Dx + TMZ QDs group (p<0.05). Cells treated with CdS/Dx QDs showed a reduced number of cells in apoptosis. These findings correlated with previously shown images, which evinced the presence of membrane blebbing and the formation of apoptotic bodies in those cells treated with TMZ alone, as well as those bioconjugated with CdS/Dx QDs.

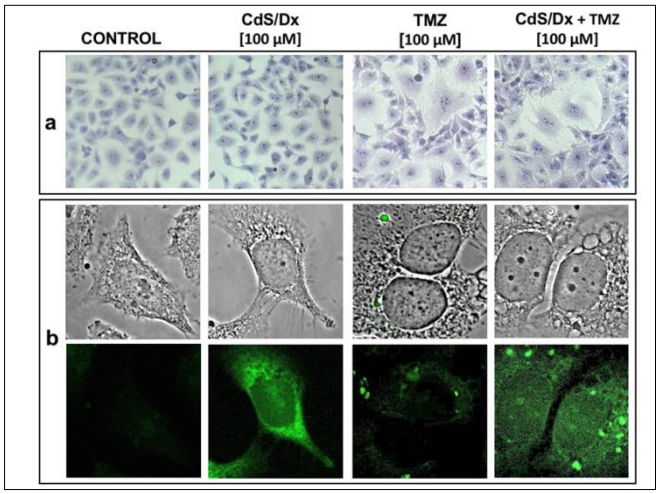

Figure 4 Nuclear integrity and cellular uptake of CdS/Dx+TMZ QDs in C6 glioma cell line. Cells were treated with CdS/Dx QDs [100 μM], TMZ [100 μM] and CdS/Dx +TMZ [100 μM] for 24 h. (a) Samples were stained with Giemsa to evaluate the effect on nuclear integrity using microscopy (×20); (b) Samples were observed with a confocal microscope and the cell internalization of QDs was analyzed. Fluorescence microscopy (×40 magnification). Scale bar=50 μm. These are representative results of at least three independent experiments (n = 3)

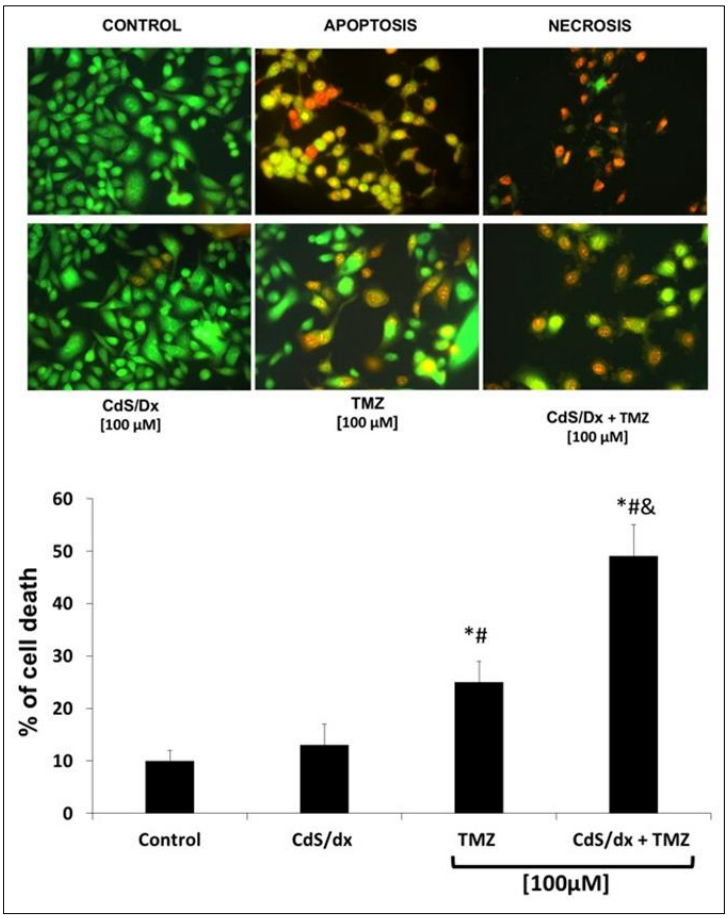

Figure 5 Cell death induced by CdS/Dx+TMZ QDs in C6 glioma cell line. Cells were treated with CdS/Dx QDs, TMZ and CdS/Dx +TMZ (100 µM) for 72 h, stained with AO/EtBr and analyzed using fluorescence microscopy (20X magnification). Cells exposed to 1 µL/mL of 30 % H_2O_2 for 2 h were used as indicators of apoptosis; cells exposed to 100 °C for 5 min were used as indicators of necrosis; and non-treated cells were used as negative control. Results are expressed as percentage of cell death as compared to control group. Data are presented as the mean ± SD of at least three independent experiments. *p <0.05 as compared to control group; # p<0.05 as compared to CdS/Dx QDs and & p<0.05 as compared with TMZ group

4 Discussion

In this work, we bioconjugated CdS-Dx + TMZ QDs and carried out an optical characterization of these QDs using different techniques. We also evaluated their pharmacological activity. The results show that CdS-Dx/QDs bioconjugated with TMZ distribute in the cytoplasm and nucleus of glioma cells, and the pharmacological effects of drugs can be observed and enhanced.

For almost two decades, TMZ has been one of the therapeutic agents employed in the treatment of malignant gliomas and is associated with a higher rate of patient survival [28]. However, TMZ has two disadvantages:1) it undergoes spontaneous hydrolysis in brain tissue and, as a consequence, low concentrations are to be found in the target site; 2) tumor cells can generate resistance to TMZ in tumor tissue, promoting tumor recurrence with a more aggressive phenotype [29, 13]. For these reasons, several experimental strategies have sought to improve delivery methods and therapeutic efficacy.

A series of nanomaterials with different size, structure, surface characteristics and coatings have emerged that favor the delivery of drugs in the brain tissue [27, 30, 31]. Nanomaterials aid effectiveness and reduce drug resistance by improving drug transport, acting as extended delivery systems and increasing drug concentration at the target site. Given the characteristics of TMZ, nano delivery systems should focus on facilitating transport and increasing drug concentrations in brain tumoral tissue, thus extending TMZ mean residence in the brain and boosting effectiveness.

QDs are non-polymeric nanomaterials that have become very useful in biomedicine because they can be coated with a great variety of molecules that improve their biocompatibility and bioactivity [32-34]. Given the variety of coatings and their small size, QDs can be easily conjugated with drugs and bioactive molecules while maintaining photostability. They can easily cross the cell membrane and deliver the therapeutic agent in target sites in addition to easing cellular monitoring through photoluminesce. This research used CdS QDs coated with dextrin, which have been shown to be innocuous in in vivo models [20-22]. Our AFM results showed that CdS-Dx + TMZ QDs were spherical in shape, had an average particle size of 6.5 nm, and the pharmacological studies demonstrated they caused higher mortality among glioma cells than TMZ alone. In addition, their fluorescence emission allowed us to monitor their pathway into the cell. The treatment of glioma cells with CdS/Dx + TMZ QDs induced cell death, which suggests that the drug probably interacted with DNA.

Several nanostructures have been studied for the delivery of TMZ alone or its codelivery with other molecules. These include polymer-based nanosystems (such as polymeric nanoparticles, dendrimers, polymeric micelles), and lipid based nanosystems (liposomes, solid lipid nanoparticles, and nanostructured lipid carriers) [35, 36]. However, there are only two reports where TMZ has been conjugated with QDs. In one, the use of small carbon QDs (2.6-3.5 nm) loaded with TMZ/epirubicin produced high mortality in glioblastoma cell lines [37]. In the other, nanofibers of carbon dots (chitosan-polyethyene-carbon QDs/carboxymethyl cellulose-alcohol) were prepared to ensure effective and sustained TMZ delivery in a glioblastoma cell line. The use of this nanofiber also made it possible to monitor cellular distribution and identify apoptotic cells via QD fluorescence [38].

Several studies have used other types of non-polymeric nanoparticles. For instance, TMZ has been conjugated with gold nanoparticles/L-Aspartate (GNPs) with a diameter of 55 nm. GNPs-conjugated TMZ delivered a cell death rate of up to 50% compared to TMZ alone [39]. Another report studied the anticancer effects of TMZ- indocyanine green in Fe_3O_4 magnetic nanoparticles in a human GBM cell line. Those nanoparticles were spherical in shape with an average size of 13 nm and reduced the viability of glioma cells in 96% [40]. However, those studies could not monitor the cells.

Previous studies have shown that TMZ causes apoptosis in human and rat glioma cells via activation of the MAPK signaling pathway, the inhibition of STAT3, and cell cycle arrest [41-43]. Present results agree with those reports, and rat glioma cells treated with CdS/Dx+ TMZ QDs showed a reduction in cell proliferation at 10 and 100 μM, with the latter concentration resulting in more significant inhibition. On the other hand, the percentage of apoptotic cells was almost twice as much in the CdS/Dx+ TMZ QD treated groups than those using TMZ alone. These findings also correlate with the morphological changes in the cells, including the membrane blebbing and presence of apoptotic bodies shown in confocal microphotographs. Present results demonstrate that the QDs allowed for a highly concentrated drug delivery, which can be seen in the presence of high photoluminescence in nuclei, as well as the accompanying therapeutic efficacy. Studies using GNP conjugated TMZ also found an increase (90%) of apoptosis in glioma-derived cancer stem cells when compared to TMZ alone (42%) [44].

The use of quantum dots in biomedicine has been delayed due to the risks they present. Most QDs contain elements that could release extremely toxic ions [45]. The pharmaceutical industry requires that QD-based nanocarriers meet the requirements of vehicles and excipients used in drug formulations and allow for better administration and dosage. Unfortunately, several QDs fail to meet these requirements because they possess a certain degree of toxicity and there is a lack of safety studies. The use of nanocarriers for the treatment of brain tumors entails rigorous studies involving biodisposition, biodegradability and biocompatibility. Today, clinical trial-related developments of nanotechnology-based materials used in the treatment of glioblastoma include the use of liposomes, and there have been no clinical trials using QDs [46]. Previous studies by this group have shown that CdS/Dx cross the blood-brain barrier and can reach brain tissue, where they have a mean residence time of 8.4 days in rats and do not produce morphological alterations of said tissue [47].

5 Conclusion

CdS/Dx QDs have the potential to be used as nanocarriers for drug delivery targeted at brain tissue. Present results demonstrate that CdS/Dx+ TMZ QDs may improve the efficacy of drug delivery while also providing fluorescence imaging of glioma cells. Therefore, they could be simultaneously used as drug delivery system and cell monitoring system for the treatment of GBM and other brain tumors.

Compliance with ethical standards

Acknowledgement

The authors also wish to thank Q.F.B. Xochitl Alvarado Affantranger at the National Laboratory of Advanced Microscopy, UNAM

Disclosure of conflict of interest

The authors have no conflicts of interest.

Funding

This work was funded by CONACyT via project Fronteras 74884 and DGAPA-PAPIIT via project IG100920.

References

[1] De Sanctis A, Mehew JD, Craciun MF, Russo S. Graphene-Based Light Sensing: Fabrication, Characterisation, Physical Properties and Performance. Materials (Basel). 2018 Sep; 11(9): 1762. https://doi.org/10.3390/ma11091762.

[2] Georgakilas V, Otyepka M, Bourlinos AB, Chandra V, Kim N, Kemp KC, et al. Functionalization of graphene: covalent and non-covalent approaches, derivatives and applications. Chem Rev. 2012 Nov;112(11):6156-214. https://doi.org/10.1021/cr3000412.

[3] Li SD, Huang L. Stealth nanoparticles: high density but sheddable PEG is a key for tumor targeting. J Control Release. 2010 Aug;145(3):178-81. https://doi.org/10.1016/j.jconrel.2010.03.016.

[4] Karabasz A, Bzowska M, Szczepanowicz K. Biomedical Applications of Multifunctional Polymeric Nanocarriers: A Review of Current Literature. Int J Nanomedicine. 2020 Nov;15:8673- 8696. https://doi.org/10.2147/IJN.S231477.

[5] Mi P. Stimuli-responsive nanocarriers for drug delivery, tumor imaging, therapy and theranostics. Theranostics. 2020 Mar;10(10):4557-4588. https://doi.org/10.7150/thno.38069.

[6] Su S, M Kang P. Recent Advances in Nanocarrier-Assisted Therapeutics Delivery Systems. Pharmaceutics. 2020 Sep;12(9):837. https://doi.org/10.3390/pharmaceutics12090837.

[7] Tandale P, Choudhary N, Singh J, Sharma A, Shukla A, Sriram P, et al, Fluorescent quantum dots: An insight on synthesis and potential biological application as drug carrier in cancer. Biochem Biophys Rep. 2021 Mar; 26: 100962. https://doi.org/10.1016/j.bbrep.2021.100962.

[8] Wang J, Li Y, Nie G. Multifunctional biomolecule nanostructures for cancer therapy. Nat Rev Mater. 2021;6(9):766-783. https://doi.org/10.1038/s41578-021-00315-x.

[9] Wagner AM, Knipe JM, Orive G, Peppas NA. Quantum dots in biomedical applications. Acta Biomater. 2019 Aug;94:44-63. https://doi.org/10.1016/j.actbio.2019.05.022.

[10] Chen D, Liu X, Lu X, Tian J. Nanoparticle drug delivery systems for synergistic delivery of tumor therapy. Front Pharmacol. 2023 Feb;14:1111991. https://doi.org/10.3389/fphar.2023.1111991.

[11] Wang X, Li C, Wang Y, Chen H, Zhang X, Luo C, et al. Smart drug delivery systems for precise cancer therapy. Acta Pharm Sin B. 2022 Nov;12(11):4098-4121. https://doi.org/10.1016/j.apsb.2022.08.013.

[12] Adepu S, Ramakrishna S. Controlled Drug Delivery Systems: Current Status and Future Directions. Molecules. 2021 Sep;26(19):5905. https://doi.org/10.3390/molecules26195905.

[13] Ortiz R, Perazzoli G, Cabeza L, Jiménez-Luna C, Luque R, Prados J, et al. Temozolomide: An Updated Overview of Resistance Mechanisms, Nanotechnology Advances and Clinical Applications. Curr Neuropharmacol. 2021;19(4):513-537. https://doi.org/10.2174/1570159X18666200626204005.

[14] Peer D, Karp JM, Hong S, Farokhzad OC, Margalit R, Langer R. Nanocarriers as an emerging platform for cancer therapy. Nat Nanotechnol. 2007 Dec;2(12):751-60. https://doi.org/10.1038/nnano.2007.387.

[15] Arakawa Y, Mineharu Y, Uto M, Mizowaki T. Optimal managements of elderly patients with glioblastoma. Jpn J Clin Oncol. 2022 Aug 5;52(8):833-842. doi: 10.1093/jjco/hyac075. Erratum in: Jpn J Clin Oncol. 2022 Nov;52(11):1358. https://doi.org/10.1093/jjco/hyac075.

[16] Wang T, Pickard AJ, Gallo JM. Histone Methylation by Temozolomide; A Classic DNA Methylating Anticancer Drug. Anticancer Res. 2016 Jul;36(7):3289-99.

[17] Przystal JM, Waramit S, Pranjol MZI, Yan W, Chu G, Chongchai A, et al. Efficacy of systemic temozolomide-activated phage-targeted gene therapy in human glioblastoma. EMBO Mol Med. 2019 Apr;11(4):e8492. https://doi.org/10.15252/emmm.201708492.

[18] Ramalho MJ, Andrade S, Coelho MÁN, Loureiro JA, Pereira MC. Biophysical interaction of temozolomide and its active metabolite with biomembrane models: The relevance of drug-membrane interaction for Glioblastoma Multiforme therapy. Eur J Pharm Biopharm. 2019 Mar;136:156- 163. https://doi.org/10.1016/j.ejpb.2019.01.015.

[19] Belter A, Barciszewski J, Barciszewska AM. Revealing the epigenetic effect of temozolomide on glioblastoma cell lines in therapeutic conditions. PLoS One. 2020 Feb;15(2):e0229534. https://doi.org/10.1371/journal.pone.0229534.

[20] Gutiérrez-Sancha I, Reyes-Esparza J, Rodríguez-Fragoso P, García-Vázquez F, Rodríguez-Fragoso L. Bright Green Emitting Maltodextrin Coated Cadmium Sulfide Quantum Dots as Contrast Agents for Bioimaging: A Biocompatibility Study. Int J Nanomed Nanosurg. 2015; 1(2): 1-10. https://doi.org/10.16966/2470-3206.107.

[21] Reyes-Esparza J, Martínez-Mena A, Gutiérrez-Sancha I, Rodríguez-Fragoso P, de la Cruz GG, Mondragón R, et al. Synthesis, characterization and biocompatibility of cadmium sulfide nanoparticles capped with dextrin for in vivo and in vitro imaging application. J Nanobiotechnology. 2015 Nov;13:83. https://doi.org/10.1186/s12951-015-0145-x.

[22] Rodríguez-Fragoso P, Reyes-Esparza J, León-Buitimea A, Rodríguez-Fragoso L. Synthesis, characterization and toxicological evaluation of maltodextrin capped cadmium sulfide nanoparticles in human cell lines and chicken embryos. J Nanobiotechnology. 2012 Dec;10:47. https://doi.org/10.1186/1477-3155-10- 47.

[23] Gutiérrez-Sancha I, Reyes-Esparza J, Rodríguez-Fragoso P, Rodríguez-Fragoso L. Pharmacokinetic of maltodextrin coated cadmiun sulfide quantum dots in rats. Nanomedicine & Biotherapeutic Discovery. 2016; 6(1):1000139. https://doi.org/10.4172/2155-983X.1000139.

[24] Gonzalez de la Cruz G, Rodríguez Fragoso P, Mastache-juarez A, Reyes-Esparza J, Rodríguez-Fragoso L. Doxorubicin-bioconjugated cadmiun sulfide dextrin quantum dots for imaging cells. Indian J Pharm Sci-2020; 82 (2); 230-241. https://doi.org/10.36468/pharmaceutical-sciences.643.

[25] Wang HZ, Chang CH, Lin CP, Tsai MC. Using MTT viability assay to test the cytotoxicity of antibiotics and steroid to cultured porcine corneal endothelial cells. J Ocul Pharmacol Ther. 1996 Spring;12(1):35-43. https://doi.org/10.1089/jop.1996.12.35.

[26] Boya P, Andreau K, Poncet D, Zamzami N, Perfettini JL, Metivier D, et al. Lysosomal membrane permeabilization induces cell death in a mitochondrion-dependent fashion. J Exp Med. 2003 May;197(10):1323-34. https://doi.org/10.1084/jem.20021952.

[27] Khosa A, Krishna KV, Dubey SK, Saha RN. Lipid Nanocarriers for Enhanced Delivery of Temozolomide to the Brain. Methods Mol Biol. 2020;2059:285-298. https://doi.org/10.1007/978-1-4939-9798-5_15.

[28] Thomas A, Tanaka M, Trepel J, Reinhold WC, Rajapakse VN, Pommier Y. Temozolomide in the Era of Precision Medicine. Cancer Res. 2017 Feb;77(4):823-826. https://doi.org/10.1158/0008-5472.CAN-16-2983.

[29] Cruz JVR, Batista C, Afonso BH, Alexandre-Moreira MS, Dubois LG, Pontes B, et al. Obstacles to Glioblastoma Treatment Two Decades after Temozolomide. Cancers (Basel). 2022 Jun;14(13):3203. https://doi.org/10.3390/cancers14133203. [

[30] Liang P, Shi H, Zhu W, Gui Q, Xu Y, Meng J, et al. Silver nanoparticles enhance the sensitivity of temozolomide on human glioma cells. Oncotarget. 2017 Jan;8(5):7533- 7539. https://doi.org/10.18632/oncotarget.13503.

[31] Kudarha RR, Sawant KK. Chondroitin sulfate conjugation facilitates tumor cell internalization of albumin nanoparticles for brain-targeted delivery of temozolomide via CD44 receptor-mediated targeting. Drug Deliv Transl Res. 2021 Oct;11(5):1994-2008. https://doi.org/10.1007/s13346-020-00861-x.

[32] Zhang M, Bishop BP, Thompson NL, Hildahl K, Dang B, Mironchuk O, et al. Quantum Dot Cellular Uptake and Toxicity in the Developing Brain: Implications for Use as Imaging Probes. Nanoscale Adv. 2019 Sep;1(9):3424-3442. https://doi.org/10.1039/C9NA00334G.

[33] Gao H. Progress and perspectives on targeting nanoparticles for brain drug delivery. Acta Pharm Sin B. 2016 Jul;6(4):268-86. https://doi.org/10.1016/j.apsb.2016.05.013.

[34] Agarwal R, Domowicz MS, Schwartz NB, Henry J, Medintz I, Delehanty JB, et al. Delivery and tracking of quantum dot peptide bioconjugates in an intact developing avian brain. ACS Chem Neurosci. 2015 Mar;6(3):494-504. https://doi.org/10.1021/acschemneuro.5b00022. [

[35] Iturrioz-Rodríguez N, Sampron N, Matheu A. Current advances in temozolomide encapsulation for the enhancement of glioblastoma treatment. Theranostics. 2023 May;13(9):2734- 2756. https://doi.org/10.7150/thno.82005.

[36] Bozzato E, Bastiancich C, Préat V. Nanomedicine: A Useful Tool against Glioma Stem Cells. Cancers (Basel). 2020 Dec;13(1):9. https://doi.org/10.3390/cancers13010009.

[37] Hettiarachchi SD , Graham RM , Mintz KJ , Zhou Y , Vanni S , Peng Z , et al. Triple conjugated carbon dots as a nano-drug delivery model for glioblastoma brain tumors. Nanoscale. 2019 Mar;11(13):6192- 6205. https://doi.org/10.1039/c8nr08970a.

[38] Shamsipour M, Mansouri AM, Moradipour P. Temozolomide Conjugated Carbon Quantum Dots Embedded in Core/Shell Nanofibers Prepared by Coaxial Electrospinning as an Implantable Delivery System for Cell Imaging and Sustained Drug Release. AAPS PharmSciTech. 2019 Jul;20(7):259. https://doi.org/10.1208/s12249-019-1466-0.

[39] Orza A, Soriţău O, Tomuleasa C, Olenic L, Florea A, Pana O, et al. Reversing chemoresistance of malignant glioma stem cells using gold nanoparticles. Int J Nanomedicine. 2013;8:689- 702. https://doi.org/10.2147/IJN.S37481.

[40] Kwon YM, Je JY, Cha SH, Oh Y, Cho WH. Synergistic combination of chemo-phototherapy based on temozolomide/ICG-loaded iron oxide nanoparticles for brain cancer treatment. Oncol Rep. 2019 Nov;42(5):1709-1724. https://doi.org/10.3892/or.2019.7289.

[41] Kobylinska LI, Klyuchivska OY, Grytsyna II, Finiuk N, Panchuk RR, Starykovych MO, et al. Differential pro-apoptotic effects of synthetic 4-thiazolidinone derivative Les-3288, doxorubicin and temozolomide in human glioma U251 cells. Croat Med J. 2017 Apr;58(2):150-159. https://doi.org/10.3325/cmj.2017.58.150.

[42] Lee SY. Temozolomide resistance in glioblastoma multiforme. Genes Dis. 2016 May;3(3):198- 210. https://doi.org/10.1016/j.gendis.2016.04.007.

[43] Günther W, Pawlak E, Damasceno R, Arnold H, Terzis AJ. Temozolomide induces apoptosis and senescence in glioma cells cultured as multicellular spheroids. Br J Cancer. 2003 Feb;88(3):463- 9. https://doi.org/10.1038/sj.bjc.6600711.

[44] Petrenko D, Chubarev V, Syzrantsev N, Ismail N, Merkulov V, Sologova S, et al. Temozolomide Efficacy and Metabolism: The Implicit Relevance of Nanoscale Delivery Systems. Molecules. 2022 May;27(11):3507. doi: 10.3390/molecules27113507. https://doi.org/10.3390/molecules27113507. [

[45] Cheng Z, Li M, Dey R, Chen Y. Nanomaterials for cancer therapy: current progress and perspectives. J Hematol Oncol. 2021 May;14(1):85. https://doi.org/0.1186/s13045-021-01096-0.

[46] US Food and Drug Administration website [http://www.accessdata.fda.gov/]

[47] Gonzalez De La Cruz G, Gómez-Cansino R, Rodríguez-Fragoso P, Paola JaimescháveZ J, Barbosa-Ray AL, Reyes-Esparza J, et al. Disposition and Biocompatibility of Dextrin-coatedCadmium Sulphide Nanoparticles after a Single Dose and Multiple Doses in Rats Indian J Pharm Sci. 2019; 81(5): 876-884. https://doi.org/10.36468/pharmaceutical-sciences.582.